PHYSICAL REVIEW B **83**, 245425 (2011)

Sensing surface states of Bi films by magnetotransport

D. Lükermann,[1] S. Sologub,[2] H. Pfnür,[1] and C. Tegenkamp[1,*]

[1]*Institut für Festkörperphysik, Leibniz Universität Hannover, Appelstraße 2, D-30167 Hannover, Germany*

[2]*Institute of Physics, National Academy of Sciences of Ukraine, Nauky Avenue 46, 03028 Kyiv, Ukraine*

(Received 11 February 2011; revised manuscript received 16 May 2011; published 27 June 2011)

Macroscopic magnetotransport measurements at Bi films grown epitaxially on Si(111) substrates have been carried out at 10 K. The magnetoconductance curves reveal two characteristic regimes, which are assigned to magnetotransport by surface and bulk states, respectively. In contrast to bulk, backscattering, i.e., weak localization, is strongly restricted for the charge carriers in the spin-polarized surface bands, and a classical magnetoresistance behavior was found. While the surface-state conductivity was found to be as high as $4 \times 10^{-4}\ \Omega^{-1}/\square$, the bulk conductivity is extremely low, possibly due to quantum confinement of the bulk band structure.

DOI: 10.1103/PhysRevB.83.245425 PACS number(s): 73.50.−h, 68.55.J−, 73.61.−r

Electronic transport in thin metallic films is more in the focus of current interest, since the ability to contact these thin films and even monolayers in a controlled manner has opened unique possibilities, and it allows us to probe inherent instabilities in low-dimensional electron gases by transport measurements.[1,2]

When thin-film structures are considered, both surface and interface effects become important. In this respect, Bi has already been extensively studied.[3–6] This material provides a semimetallic band structure with an extremely long Fermi wavelength ($\lambda_F \approx 30$ nm) and with high carrier mobilities, making quantum size effects, e.g., the predicted semimetal-to-semiconductor transition, accessible.[4] Surface states of the (111)-oriented surface lead to a strongly enhanced electron concentration at E_F compared to the bulk. As a consequence, transport properties in epitaxially grown Bi films on Si(111) are to a large extent determined by the surface states.[7,8]

There are only a few examples in the literature where magnetotransport has been applied to ultrathin films with explicit consideration of surfaces and interfaces.[9,10] In this context, epitaxially grown Bi films with strongly spin-polarized surface states[11] open unique pathways for magnetotransport. For example, weak localization effects were found first in Bi films[12] and, for thin Bi films, even weak antilocalization (WAL) effects became apparent and were correlated with the prevailing strong spin-orbit coupling (SOC) in Bi. However, for bulk Bi WAL effects are not expected, since there is no lifting of the spin degeneracy because of inversion symmetry. Hence, the WAL effect was interpreted to originate from the scattering of bulk electrons at the interface or surface states.[13,14] An interesting question arises now for transport along the surface. Electrons originating from spin-polarized states cannot be backscattered easily because spin umklapp is required. For Bi(111), indeed, strongly reduced backscattering was found by analyzing the standing wave patterns with a scanning tunneling microscope (STM).[15] Therefore, weak localization (or antilocalization) for electronic transport in the surface states is strongly reduced and should become important at first in the limit of ultralong elastic mean-free-path lengths.

In this paper we show that the measurement of magnetotransport allows a quantitative determination of transport relevant parameters of both electrons and holes in surface and bulk states. The magnetoconductance curve reveals a dip structure at low magnetic fields, which can be described by WAL of bulk electrons using the Hikami theory. The shoulder at higher magnetic fields is explained by classical magneto-surface transport, in agreement with the considerations from above.

For the conductivity measurements, low-doped Si(111) samples were used as substrates for the film growth. Details about the fabrication of reliable contacts as well as of the cleaning procedures are described elsewhere.[16] Bi and Pb were evaporated out of ceramic crucibles, and the amount was controlled by quartz microbalances. Bi films were grown at room temperature, followed by annealing to 400 K for several minutes. Further details can be found elsewhere.[17,18] The Bi coverage was calibrated by the $\sqrt{3} \times \sqrt{3}$ β phase on Si(111) (Ref. 19) and by recording oscillations in conductance during the evaporation of Bi at 10 K on annealed Bi films. For indexing the Bi planes, the rhombohedral notation was used;[18] i.e., the surface normal coincides with the ⟨111⟩ direction, and the coverage is given in bilayers ($1\ \text{BL} = 1.14 \times 10^{15}\ \text{atoms/cm}^2$). For magnetotransport measurements, the prepared Bi films were transferred *in situ* into a split-coil magnet (±4 T).

A low-energy electron diffraction (LEED) pattern of an epitaxially grown 4-BL-thick Bi film on Si(111) is shown in Fig. 1. Besides the first-order spots of the Bi film, ring structures with various diameters are visible, indicating growth of different crystallographic orientations with rotational disorder. The inner-ring structure (r1) consists in fact of two rings, which can be assigned to the pseudocubic surface cell of the Bi(110) surface structure growing at the interface.[17] The outer ring (r2) is located at 101.3% surface Brillouin zone (SBZ) and matches perfectly with the interlayer spacing of the Bi{011} planes (3.28 Å). According to Ref. 17, the thickness of the Bi film with this orientation is at least 3–4 BL. On top, the Bi grows in the (111) orientation, as can be seen by the first-order spots appearing on the ring denoted by r3. In general, the ring structures reflect a pronounced rotational disorder of the Bi film. More details about the film growths and the formation of the allotropic phase at the interface can be found in Refs. 17 and 18. The coexistence of the different allotropic phases is no longer visible in LEED for higher coverages. As demonstrated in the inset of Fig. 1, for 7 BL only the stable rhombohedral

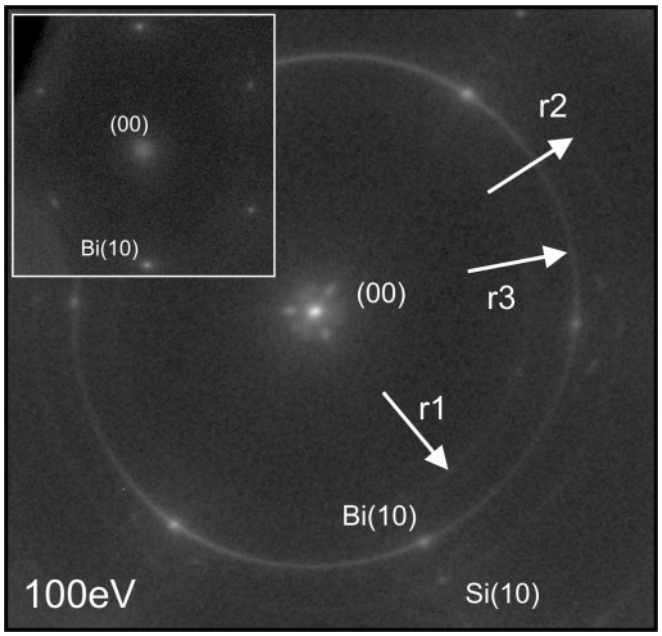

FIG. 1. LEED pattern of 4-BL Bi grown epitaxially on Si(111). The image is slightly distorted due to residual magnetization of the LEED instrument after performing magnetotransport in the same system. The different ring structures (r1, r2, r3) are explained in the text. For thicker films (7 BL, see the inset) only a single-domain (111) texture of the surface is visible in LEED.

orientation can be seen. Furthermore, the rotational disorder of the surface is strongly reduced with increasing film thickness.

The transport properties of the Bi film and of the surface were probed simultaneously using magnetotransport measurements. Figure 2 shows the relative magnetoconductance

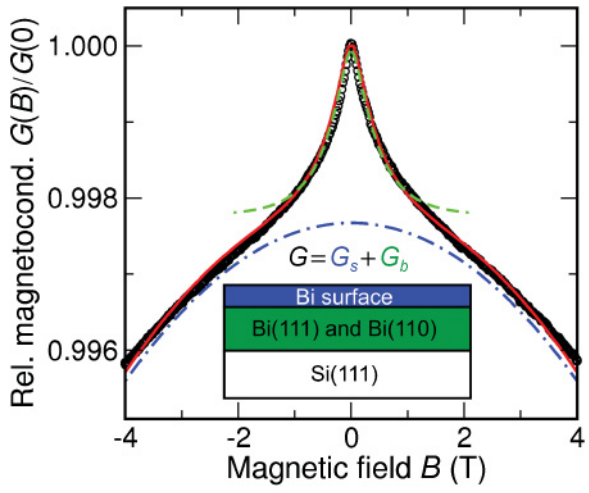

FIG. 2. (Color online) Relative magnetoconductance $G(B)/G(0)$ of the Bi film (7 BL) shown in the inset of Fig. 1. The MR analysis has revealed that the changes in conductance in the regime of low and high magnetic fields can be attributed to transport through the surface states [dashed-dotted (blue) line, classical MR, G_s] and bulk [dashed (green) line, WAL, G_b]. For better visibility, both contributions are slightly shifted. Absolute values are discussed in context with Fig. 3.

curve, exemplarily, for a 7-BL Bi film. The relative change in magnetoconductance is below 1%, i.e., far away from that reported for bulk systems.[20,21] This shows already that the mobilities of both electrons and holes are significantly lower in Bi thin-film structures than in a single-crystal material. As we will show in the following, the pronounced peak-shoulder structure in the $G(B)$ curves is related to bulk and surface-state-related transport, respectively. This separation is evident from the systematic variation of the film thickness and from adsorption experiments. While the dip is explained by WAL, in agreement with previous investigations, the shoulder can be explained by the classical magnetoresistance effect, i.e., an increase in resistance due to extended electron paths in the presence of transversally applied magnetic fields.

The magnetoconductance curves were analyzed in detail using the two-carrier model for the surface-state-related transport.[22] For the given electron and hole mobilities (μ_n and μ_p) and the ratio $c = p/n$, where p and n denote the hole and electron concentration, respectively, the surface magnetoconductance $G_s(B)$ can be expressed by

$$G_s(B) = G_s(0)\frac{1+(1-c)^2\frac{\mu_n^2\mu_p^2}{(\mu_n+c\mu_p)^2}B^2}{1+\mu_n\mu_p\frac{\mu_p+c\mu_n}{\mu_n+c\mu_p}B^2}.$$

After substraction of this Drude background, the remaining dip structure at low magnetic fields can be satisfactorily modeled within the framework of weak (anti)localization elaborated by Hikami and co-workers.[23] The magnetoconductance of the bulk-related electrons is given by $G_b(B) = G_b(0) - G_{00}[f(\frac{B_o+B_{so}}{B}) - \frac{3}{2}f(\frac{4/3B_{so}+B_i}{B}) + \frac{1}{2}f(\frac{B_i}{B})]$, with $f(B_\nu/B) = \Psi(1/2 + B_\nu/B) - \ln(B_\nu/B)$, where Ψ is the digamma function, $G_{00} = e^2/(2\pi^2\hbar)$, and $G_b(0)$ is the bulk conductance at zero magnetic field. B denotes the externally applied magnetic field, and the B_ν, $\nu = i,o,so$ are defined as $B_\nu = \hbar n/(4ev_F^2\tau_o\tau_\nu)$. For a given Fermi velocity v_F of the electrons with charge e, all essential scattering parameters τ_i (inelastic), τ_o (elastic), and τ_{so} (spin orbit) can be determined.

Figure 2 shows exemplarily for a 7-BL-thick Bi film the decomposition into the two characteristic regimes. It should be noted that for the bulk contribution only one type of carrier is taken into account (cf. Ref. 14). The small amplitude of this peak is related to the small conductance of the bulk and is caused by confinement.[6] Furthermore, for thin films at low temperatures the majority carriers are holes.[6] Therefore, the description of the bulk contribution with only one type of carrier is justified. This no longer holds for the surface states, as seen by photoemission,[11] and both types of carriers were considered in the classical magnetoresistance (MR) theory. The shoulder cannot be described by the theory of weak (anti)localization, as is also obvious from the curvature of the shoulder.

The identification of the peak and the shoulder with film- and surface-dominated transport channels, respectively, is evidenced by a systematic variation of the Bi film thickness with an increasing number of layers [Figs. 3(c)–3(e)]. The absolute height of the peak in the magnetoconductance curves at low fields remains unchanged, but the slopes of the shoulders of the magnetoconductance curves increase gradually in the regime of high magnetic fields with increasing film thickness. Since the slope is strongly influenced by the mobility of the

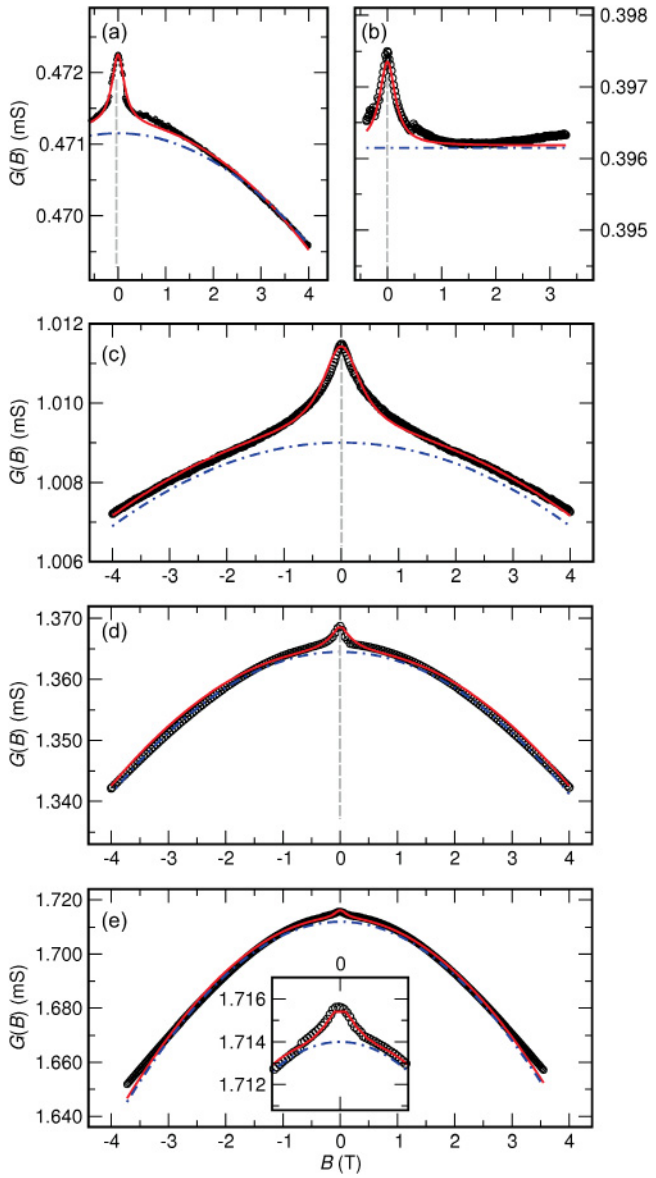

FIG. 3. (Color online) Magnetoconductance curves obtained for (a) 5, (c) 7, (d) 15, and (e) 22 BL. All measurements were performed at 10 K. The inset magnifies the peak visible for a 22-BL film. (b) Adsorption of ∼0.5 ML Pb on a 5-BL film leads to strong reduction of the conductance and the mobility. The dashed-dotted lines represent the contributions of surface magnetoconductance.

carriers, the scattering of electrons within the surface states is reduced. This is compatible with LEED investigations showing that the (111) textured grains increase, i.e., the rotational disorder is decreasing with increasing Bi film thickness.[18]

In addition, the change in magnetoconductance found after adsorption of 0.5 monolayers (ML) Pb at 10 K on a 5-BL film support this assignment: As shown in Fig. 3(b), the conductance at zero magnetic field decreases by ≈0.08 mS (cf. Table I), and the MR effect in the regime of large magnetic fields is reduced almost to zero. In contrast, the peak at low fields remains almost unchanged, emphasizing the bulk character. In the particular case shown, the surface conductance even increases again at fields ∼2 T, possibly due to weak localization effects for electrons in surface bands, since the Pb adatoms act as scatterers and annihilate to some extent the restrictions regarding backscattering. In any case, it is noteworthy that classical MR theory describes the surface contribution extremely well, as also found recently by micro-four-point-probe magnetotransport measurements.[24] As mentioned above, in our case, the reduction of weak localization effects is expected since backscattering is restricted for charge carriers in spin-polarized surface states.

The results obtained from the MR analysis are summarized in Table I: Compared to the contribution from the surface, the bulk conductance of the thin film is almost three orders of magnitude smaller, as directly obvious from the small amplitude of the peak at zero magnetic field. This contrasts with the conductance expected for an infinite bulk system. For instance, using the ideal bulk resistivity of Bi (106.8 $\mu\Omega$ cm), the conductance is expected to be three orders of magnitude higher for a 5-BL film.

With increasing film thickness, the elastic scattering rate $1/\tau_0$ decreases. This is the result of the homogeneous rhombohedral Bi phase, but the bulk conductance is still extremely small. The calculation of carrier mobilities has some uncertainty as the exact electronic structure for these thin films is not clear. In the case of the 22-BL film, e.g., the mobilities deduced from the elastic scattering times are of the order of 0.5 $m^2/V\,s$ assuming effective hole masses $\sim 0.01 m_e$. Such mobility values are expected for thin films and are in reasonable agreement with other transport data.[6]

A temperature-dependent transport measurement is shown in Fig. 4(a), exemplarily for a 15-BL film. At ∼60 K an increase in conductance is visible, which we identify with the transition into a semimetallic state of the film. Obviously, the conductance at low temperature is mainly determined by

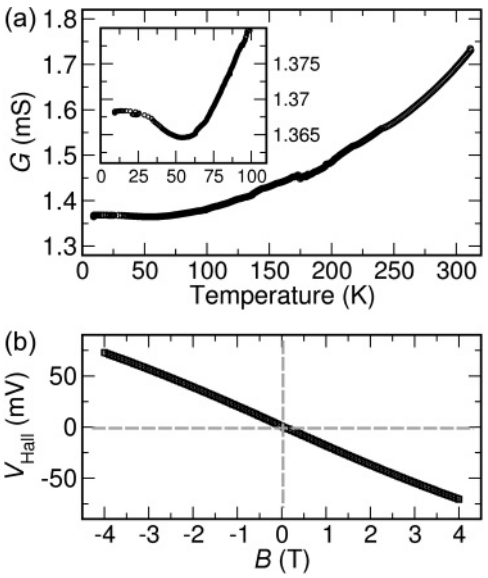

FIG. 4. (a) Conductance of a 15 BL Bi film as a function of temperature. At $T = 60$ K, activated transport sets in. At low temperatures, the conductance through the surface states is dominating. The inset shows a magnification of the low-temperature regime. (b) Hall measurements for the same Bi film. The current was 3 mA. The slope is −17.5 mV/T.

TABLE I. Mobilities, relative concentration of holes (p) and electrons (n), and characteristic scattering times (τ_i inelastic, τ_0 elastic, τ_{so} spin orbit) in surface and bulk states. $T = 10$ K.

	Surface				Bulk			
Thickness (BL)	μ_n (m^2/V s)	μ_p (m^2/V s)	$c = p/n$	$G_s(0)$ (mS)	τ_i (10^{-14} s)	τ_o (10^{-14} s)	τ_{so} (10^{-14} s)	$G_b(0)$ (mS)
5	0.033	0.005	1.3	0.47	1.5	4.0	3.9	0.001
5 + 0.5 ML Pb	0.001	(0)	0.001	0.39	1.9	5.2	4.6	0.001
7	0.028	0.004	1.2	1.0	1.3	3.7	2.7	0.002
15	0.061	0.018	1.1	1.4	1.5	9.1	3.2	0.004
22	0.104	0.030	1.0	1.7	1.1	11	7.0	0.001

electronic transport through surface states. The increase in conductance at 300 K is ∼0.35 mS and can be essentially attributed to transport through the film. For the same film thickness, a similar ratio between surface and bulk contribution was found by Hirahara *et al.*[7] in their measurements carried out at room temperature. In addition, the inset in Fig. 4(a) shows a small decrease of the conductance at ∼50 K, which can be attributed to electron-phonon scattering of the carriers within the surface states.

Finally, we discuss the surface transport properties. The results obtained from the classical MR fit are summarized in Table I as well. As mentioned in context with Fig. 3, $G_s(0)$ increases gradually as the film thickness increases. This is essentially the effect of less imperfections, e.g., rotational domains, within the surface layer of the Bi films, which is coupled with the general trend that the carrier mobilities are increasing. The surface c parameter is approximately one for all coverages considered here, i.e., both electrons and holes are contributing to the transport. The presence of both types of carriers is consistent with angle-resolved photoemission spectroscopy (ARPES) measurements, revealing electron pockets at the Γ point and hole lobes along the Γ-M direction.[11] Even more, the higher mobilities found for electrons as compared to holes correlate well with the higher curvature of electron pocket bands.

Our measurements were carried out at low temperatures with a corresponding lower (factor of 4) surface conductivity $\sigma = \ln 2/\pi G_s(0) \approx 0.4$ mS/□, compared to that reported in Ref. 7. Nevertheless, the carrier mobilities are also lower in our case, which is reasonable, because our transport measurements were performed on a macroscopic scale. The adsorption of 0.5 ML of Pb influences strongly the carrier mobilities and modifies the balance between holes and electrons of the surface states. While the conductance drops only by ∼20% due to adsorption, the electron mobility is reduced by one order of magnitude. However, considering the c parameter found from the analysis, it is evident that the surface electron concentration is increased due to the adsorption of Pb.

As deduced from dc-transport measurements, the surface carrier concentration (electrons and holes) is $\sim 10^{13}$ cm^{-2}.[7] This can be approximately corroborated by using Hall measurements, assuming that the electrons and holes from the surface bands mainly contribute. In the limit of small magnetic fields, the Hall constant can be approximated by $R_H = -\frac{1}{n|e|}\frac{\mu_n^2 - c\mu_p^2}{\mu_n + c\mu_p}$. The Hall voltage V_{Hall} is shown exemplarily for a 15-BL film in Fig. 4(b). The negative slope shows directly that the transport is dominated by electrons, i.e., that the electron mobility is dominating in the nearly charge-compensated surface bands ($c = 1.1$). From V_{Hall}, shown in Fig. 4(b) for the 15-BL film, it is obvious that the system can be described by a Hall constant over a large range. The absence of higher-order terms means that subband effects of the bulk due to confinement are not present and confirms the ultralow conductance of the bulk. In the particular case shown, a Hall constant of $R_H \approx -6$ m^2/C $= V_{\mathrm{Hall}}/I(1/B)$ is deduced from the slope using a probe current of 3 mA. This results in an electron concentration of $n \approx 4 \times 10^{12}$ cm^{-2} using the parameters shown in Table I. Thus we obtain good agreement with the electron density deduced from the electron pocket at the $\overline{\Gamma}$ point of the Bi(111) Fermi surface ($k_F = 0.05$ Å^{-1}).[15] This correlates well with the total carrier density obtained by independent surface-transport experiments.[7]

Summarizing our results, we have shown that magnetotransport is an appropriate method to discriminate between surface- and bulk-related transport properties for a given film thickness at a fixed substrate temperature. The results confirm that Bi films exhibit a large surface-state conductivity. The fact that a classical description can be successfully applied to the magnetotransport is an indirect consequence of the strong Rashba splitting of the surface states. The electrical inactivity of the underlying Bi film structure seems to be induced by confinement effects and/or allotropic disorder within the film. As it turns out, the use of thin semimetal structures seems to be a promising approach in order to effectively suppress transport through the film itself so that the surface-state conductivity becomes easily accessible in transport.

Financial support by the Deutsche Forschungsgemeinschaft (D.L.) and the DAAD (S.S.) is gratefully acknowledged.

*tegenkamp@fkp.uni-hannover.de

[1] T. Kanagawa, R. Hobara, I. Matsuda, T. Tanikawa, A. Natori, and S. Hasegawa, Phys. Rev. Lett. **91**, 036805 (2003).

[2] C. Tegenkamp, Z. Kallassy, H. Pfnür, H.-L. Günter, V. Zielasek, and M. Henzler, Phys. Rev. Lett. **95**, 176804 (2005).

[3]Yu. F. Ogrin, V. N. Lutskii, and M. I. Elinson, JETP Lett. **3**, 71 (1966).
[4]V. B. Sandomirskii, Sov. Phys. JETP **25**, 101 (1967).
[5]C. A. Hoffman, J. R. Meyer, F. J. Bartoli, A. Di Venere, X. J. Yi, C. L. Hou, H. C. Wang, J. B. Ketterson, and G. K. Wong, Phys. Rev. B **51**, 5535 (1995).
[6]C. A. Hoffman, J. R. Meyer, F. J. Bartoli, A. Di Venere, X. J. Yi, C. L. Hou, H. C. Wang, J. B. Ketterson, and G. K. Wong, Phys. Rev. B **48**, 11431 (1993).
[7]T. Hirahara, I. Matsuda, S. Yamazaki, N. Miyata, S. Hasegawa, and T. Nagao, Appl. Phys. Lett. **91**, 202106 (2007).
[8]G. Jnawali, Th. Wagner, H. Hattab, R. Möller, A. Lorke, and M. Horn-von Hoegen, e-J. Surf. Sci. Nanotechnol. **8**, 27 (2010).
[9]I. Vilfan, M. Henzler, O. Pfennigstorf, and H. Pfnür, Phys. Rev. B **66**, 241306 (2002).
[10]D. Lükermann, M. Gauch, M. Czubanowski, H. Pfnür, and C. Tegenkamp, Phys. Rev. B **81**, 125429 (2010).
[11]T. Hirahara, T. Nagao, I. Matsuda, G. Bihlmayer, E. V. Chulkov, Yu. M. Koroteev, P. M. Echenique, M. Saito, and S. Hasegawa, Phys. Rev. Lett. **97**, 146803 (2006).
[12]Y. F. Komnik, E. I. Bukhshtab, V. V. Andrievskiĭ, and A. V. Butenko, Low. Temp. Phys. **52**, 315 (1983).
[13]F. Komori, S. Kobayashi, and W. Sasaki, J. Phys. Soc. Jpn. **52**, 368 (1982).
[14]Y. F. Komnik, I. B. Bertkutov, and V. V. Andrievskiĭ, Low Temp. Phys. **31**, 326 (2005).
[15]M. C. Cottin, C. A. Bobisch, J. Schaffert, G. Jnawali, A. Sonntag, G. Bihlmayer, and R. Möller, Appl. Phys. Lett. **98**, 022108 (2011).
[16]C. Tegenkamp, D. Lükermann, S. Akbari, M. Czubanowski, A. Schuster, and H. Pfnür, Phys. Rev. B **82**, 205413 (2010).
[17]T. Nagao, J. T. Sadowski, M. Saito, S. Yaginuma, Y. Fujikawa, T. Kogure, T. Ohno, Y. Hasegawa, S. Hasegawa, and T. Sakurai, Phys. Rev. Lett. **93**, 105501 (2004).
[18]M. Kammler and M. Horn-von Hoegen, Surf. Sci. **576**, 56 (2005).
[19]R. Shioda, A. Kawazu, A. A. Baski, C. F. Quate, and J. Nogami, Phys. Rev. B **48**, 4895 (1993).
[20]J. H. Mangez, J. P. Issi, and J. Heremans, Phys. Rev. B **14**, 4381 (1976).
[21]P. B. Ahlers and R. T. Webber, Phys. Rev. **91**, 1060 (1953).
[22]A. B. Pippard, *Magnetoresistance in Metals* (Cambridge University Press, Cambridge, UK, 1989).
[23]S. Hikami, A. I. Larkin, and Y. Nagaoka, Prog. Theor. Phys. **63**, 707 (1980).
[24]N. Miyata, R. Hobara, H. Narita, T. Hirahara, S. Hasegawa, and I. Matsuda, Jpn. J. Appl. Phys. **50**, 036602 (2011).